



Shear-wave elastography: role in clinically significant prostate cancer with false-negative magnetic resonance imaging

Li-Hua Xiang^{1,2} · Yan Fang^{1,2} · Jing Wan^{1,2} · Guang Xu^{1,2} · Ming-Hua Yao^{1,2} · Shi-Si Ding^{1,2} · Hui Liu^{1,2} · Rong Wu^{1,3}

Received: 1 February 2019 / Revised: 15 April 2019 / Accepted: 13 May 2019 / Published online: 29 May 2019

© European Society of Radiology 2019

Abstract

Objectives To analyze the diagnostic value of adding SWE to MRI for the diagnosis of clinically significant prostate cancer with false-negative MRI results.

Methods This was a retrospective study of 367 patients who underwent MRI, SWE, and prostate biopsy between March 2016 and November 2018 at the Shanghai Tenth People's Hospital. Serum prostate-specific antigen (PSA) and free PSA (fPSA) were measured preoperatively. Diagnostic value and accuracy was determined for MRI alone and MRI + SWE using the receiver operator characteristic curve (ROC) analysis.

Results MRI misdiagnosed 17.9% (21/117) clinically significant prostate cancers, including 15 lesions in the peripheral zone and 6 in the central zone. Both qualitative and quantitative SWE could help detect 66.7% (10/15) significant prostate cancers with false-negative MRI, but there was no association with the Gleason score ($p > 0.05$). When considering the sextant of the peripheral zone, a significant association was not seen with histopathology in qualitative SWE ($p = 0.071$) and quantitative SWE ($p = 0.598$). Among age, PSA, fPSA, volume of the prostate gland, fPSA/PSA, and PSAD, only PSAD ($p = 0.019$) was associated with SWE results in patients with negative MRI.

Conclusions Adding SWE to MRI in patients with negative MRI for prostate examination could allow the correct diagnosis of additional patients and reduce the false-negative rate.

Key Points

- MRI plays an important role in clinically significant prostate cancers diagnosis.
- SWE plays an important role in clinically significant prostate cancers with negative MRI.
- Adding SWE to MRI in patients with negative MRI for prostate examination could allow the correct diagnosis of additional patients and reduce the false-negative rate.

Keywords Prostate cancer · Biopsy · Magnetic resonance imaging

Abbreviations

95%CI	95% confidence intervals	AP/CP	Acute/chronic prostatitis
ADC	Apparent diffusion coefficient	ASAP	Atypical small acinar hyperplasia
AHH	Atypical adenomatous hyperplasia	AUC	Area under the ROC
		BPH	Benign prostatic hyperplasia

Li-Hua Xiang and Yan Fang contributed equally to this work.

Electronic supplementary material The online version of this article (<https://doi.org/10.1007/s00330-019-06274-w>) contains supplementary material, which is available to authorized users.

✉ Rong Wu
wurong7111@163.com

¹ Department of Medical Ultrasound, Shanghai Tenth People's Hospital, Tongji University School of Medicine, No. 301, Yanchangzhong Road, Shanghai 200072, China

² Ultrasound Research and Education Institute, Tongji University School of Medicine, No. 301, Yanchangzhong Road, Shanghai 200072, China

³ Department of Ultrasound, Shanghai General Hospital, Shanghai Jiaotong University School of Medicine, Shanghai 200080, China

DCE	Dynamic contrast enhancement
DWI	Diffusion-weighted imaging
fPSA	Free PSA
HGPIN	High-grade prostate intraepithelial neoplasia
LGPIN	Low-grade prostate intraepithelial neoplasia
mp-MRI	Multiparameter magnetic resonance imaging
NCI	National Cancer Institute
NPV	Negative predictive value
NSGP	Non-specific granulomatous prostatitis
PCa	Prostate cancer
PI-RADS	Prostate Imaging Reporting and Data System
PPV	Positive predictive value
PSA	Prostate-specific antigen
PSAD	PSA density
ROC	Receiver operator characteristic
ROI	Region of interest
sPCa	Clinically significant prostate cancer
SWE	Shear-wave elastography
T1WI	T1-Weighted imaging
T2WI	T2-Weighted imaging
TRUS-Bx	Transperineal prostate biopsy guided by transrectal ultrasound
US	Ultrasound
V	Volume of the prostate gland

Introduction

Prostate cancer (PCa) is one of the most commonly diagnosed malignant tumors and the sixth leading cause of cancer deaths in men. For 2017, the National Cancer Institute (NCI) showed that there were 161,360 new cases of PCa and 26,730 deaths due to PCa in the USA, accounting for nearly one-fourth of all deaths from malignant tumors [1]. Although most PCa show little aggressiveness and with a relatively low risk of metastasis and although both the incidence and mortality decreased in the Occident, the situation in China is still pessimistic. Indeed, despite an increasing incidence due to better detection methods and cancers being detected earlier, the mortality keeps increasing [2, 3].

Multiparameter magnetic resonance imaging (mp-MRI) plays an important role in the diagnosis of clinically significant prostate cancer (sPCa). Various MRI tissue characteristics determining the sPCa risk are included in the Prostate Imaging Reporting and Data System (PI-RADS): PIRADS of 1 to 3 is more likely to be benign and a PIRADS of 4 or 5 is highly suspicious of being malignant [4]. Nevertheless, mp-MRI can miss clinically important lesions or underestimate lesion size; it has been reported that up to 58% of these lesions are missed or characterized as benign [5].

Elastography enables differentiation between benign and malignant lesions based on their stiffness [6]. Indeed, benign

lesions tend to be harder than the surrounding normal tissue, but still softer than malignant lesions [6]. Both strain elastography and shear-wave elastography (SWE) help enhance the diagnostic value of the prostate tissues [7, 8].

There are many studies about the role of MRI and/or SWE in the diagnosis of PCa, and all modalities show some misdiagnosis [7–11]. To the best of our knowledge, there are few reports about the diagnostic value of SWE for sPCa with false-negative MRI results. Therefore, the aim of the present study was to analyze the diagnostic value of adding SWE to MRI for the diagnosis of malignant prostate tissues with false-negative MRI results.

Materials and methods

Study design and patients

This retrospective study was approved by the institutional review board of the Shanghai Tenth People's Hospital. The patients were examined between March 2016 and November 2018. Oral informed consent for the use of their data for research purposes was obtained at the time of biopsy. There were 938 patients who underwent transperineal prostate biopsy guided by transrectal ultrasound (TRUS-Bx) at the Department of Medical Ultrasound, Shanghai Tenth People's Hospital. The indications for biopsy were the following: (1) abnormally elevated prostate-specific antigen (PSA) levels (> 10 ng/ml); (2) gradually increasing PSA levels by 0.75 ng/ml/year; or (3) positive digital rectal exam. All patients underwent both MRI and SWE before biopsy for suspected sPCa. Patients were excluded if they did not undergo MRI or SWE, and the PSA > 100 ng/ml. Thus, finally, 367 participants were enrolled.

Multiparametric magnetic resonance imaging

mp-MRI included T1-weighted imaging (T1WI), T2-weighted imaging (T2WI), diffusion-weighted imaging (DWI), apparent diffusion coefficient (ADC), and dynamic contrast enhancement (DCE); all were conducted using a Siemens TrioTrim Somatom 3-Tesla magnet (Siemens) with a trans-abdominal external phased-array coil. All patients underwent biopsy according to the indications above, whether the MRI was normal or abnormal.

Shear-wave elastography

Prostate ultrasound (US) and SWE examination were performed using an Aixplorer system (SuperSonic Imagine) equipped with an endocavity transrectal probe SE12-3 with high frequency (8 MHz). The patients were asked to lie in the left lateral position and to hold their knees with their hands as close to the abdomen as possible. SWE acquisitions were

performed in the transverse plane to gain the entire peripheral zone. SWE imaging was done so that each side of the prostate was scanned from the apex to the base with a very slow movement, while avoiding pre-compression of the prostate. Three SWE acquisitions were included for each side of the prostate, with a maximum elasticity scale of 70 kPa, by using a palette displaying the elasticity map by coding the soft tissue as blue and hard tissue as red. The images were stored for further analysis.

Prostate biopsy

Biopsy was performed for all participants based on the volume of the prostate and/or the MRI results, according to each participant: (1) clinically-guided biopsy; (2) MRI-US fusion targeted biopsy (MRI imaging was imported into the US system and the US image was matched with MRI using the software; thus, the suspicious lesions can be defined using US to perform the biopsy); or (3) cognitive fusion-targeted biopsy (the US image was matched with MRI or SWE by the examiner rather than by using the software).

Image analysis

All imaging was completed by one of the three sonographers with 1–2 years of experience in transrectal SWE prostate imaging. The size of the prostate was measured in the sagittal plane for longitudinal diameter (a) and in the axial for anteroposterior diameter (b) and transverse diameter (c). The volume of the prostate gland (V) was calculated according to the following formula: ($a \times b \times c \times 0.52$). The PSA density (PSAD) was calculated according to $PSAD = PSA/V$. The mp-MRI was analyzed by one of three mid-level radiologists (5–15 years of experience in prostate MRI) and reviewed by one of two radiologists with a senior professional title (> 25 years of experience) using PI-RADS, version 2 [4]. As for SWE imaging, each section plane was measured by one of two sonographers with 1–2 years of experience in prostate elastography. The measurement was performed using a round region of interest (ROI) with the same diameter of 3–5 mm (5 mm was the first consideration) in the stiffest part and the near-median region in the peripheral zone when there were no apparent lesion on US, while the ROIs were put in the suspicious and normal parts when there were suspicious lesions seen on US. SWE images were measured using both the qualitative and quantitative methods with the cut-off value ≥ 40.8 kPa, according to our previous research [12]. SWE measurements were based on the US imaging that could be helpful in identifying the position. It was regarded as positive whether the MRI or SWE showed a positive result.

Pathological examination

Patients underwent TRUS-Bx by the transperineal approach within 1 month of MRI and on the same day as SWE. The number of cores ranged from 8 to 20 on the basis of prostate volume and with or without suspicious findings on MRI. In the present study, the gold standard for diagnosis of cancer was the result from the biopsy or surgery. All histopathological examinations were performed by one of six pathologists who were blinded to the MRI and SWE findings, all with 3–15 years of experience in prostate pathology. The Gleason score was used. The positive result was defined as sPCa with the Gleason score ≥ 7 [4, 13].

Statistical analysis

All statistical analyses were performed using SPSS 22.0 (IBM). The quantitative data were expressed as means \pm standard deviation and analyzed using the Student t test or the Mann-Whitney U test, as appropriate. The categorical data were analyzed using the chi-square test or the Fisher exact test, as appropriate. Sensitivity, specificity, positive predictive value (PPV), and negative predictive value (NPV) were calculated for MRI. Receiver operating characteristic (ROC) curve analysis was performed and the area under the ROC (AUC) was calculated. For the prostate malignant tumors with negative MRI, the sensitivity, specificity, and AUC with the 95% confidence intervals (95%CI) were evaluated both for qualitative and quantitative SWE. The McNemar test and the Kappa test were conducted for the comparison of the two SWE methods. Two-sided p values < 0.05 were considered statistically significant.

Results

Characteristics of the patients

The mean age of the patients was 66.9 ± 7.5 years (range, 29–88 years; median, 67 years). Mean PSA levels were 16.09 ± 16.65 ng/ml (range, 0.43–95.12 ng/ml; median, 10.28 ng/ml). The average number of cores was 12.5 (range, 8–20). The histopathological examination showed malignancy in 36.78% (135/367) of the patients, atypical lesions in 14.17% (52/367), and benign lesions in 49.05% (180/367). Among the 135 malignant lesions, 134 were PCa: 17 with a Gleason score of 6, 71 with a Gleason score of 7, 22 with a Gleason score of 8, 23 with a Gleason score of 9, and one with a Gleason score of 10. One patient was with carcinosarcoma. Of the 52 atypical lesions, there were 25 low-grade prostate intraepithelial neoplasia (LGPIN), 10 high-grade prostate intraepithelial neoplasia (HGPIN), six atypical adenomatous hyperplasia (AHH), and 11 atypical small glandular hyperplasia (ASAP),

Table 1 Histopathological findings of all participants

Histopathology	N	%
Benign		
Benign prostatic hyperplasia (BPH)	120	32.70
Acute/chronic prostatitis (AP/CP)	58	15.80
Nonspecific granulomatous prostatitis (NSGP)	2	0.54
Atypia		
Low-grade prostate intraepithelial neoplasia (LGPIN)	25	6.81
High-grade prostate intraepithelial neoplasia (HGPIN)	10	2.72
Atypical adenomatous hyperplasia (AHH)	6	1.63
Atypical small glandular hyperplasia (ASAP)	11	3.00
P504s (+)	7	
P504s (–)	4	
Malignant		
Prostate cancer (PCa)	134	36.51
Gleason score 6	17	4.63
Gleason score 7	71	19.35
Gleason score 8	22	6.00
Gleason score 9	23	6.27
Gleason score 10	1	0.27
Carcinosarcoma	1	0.27

among which seven lesions were p504s (+). Among the 180 benign lesions, 120 were benign prostatic hyperplasia (BPH), 58 were acute/chronic prostatitis (AP/CP), and two were non-

specific granulomatous prostatitis (NSGP). The results are shown in Table 1 and Fig. 1.

mp-MRI

When performing mp-MRI, 96 positive lesions of the 117 considered were diagnosed correctly, but 21 lesions were missed; 231 negative lesions of the 250 considered were evaluated correctly, but 19 were overdiagnosed. Thus, the sensitivity was 82.05%, specificity was 92.40%, PPV was 83.48%, NPV was 91.67%, and AUC was 0.872 (95%CI 0.827–0.917) (Fig. 2). The findings by mp-MRI were significantly associated with the histopathological findings ($p < 0.001$).

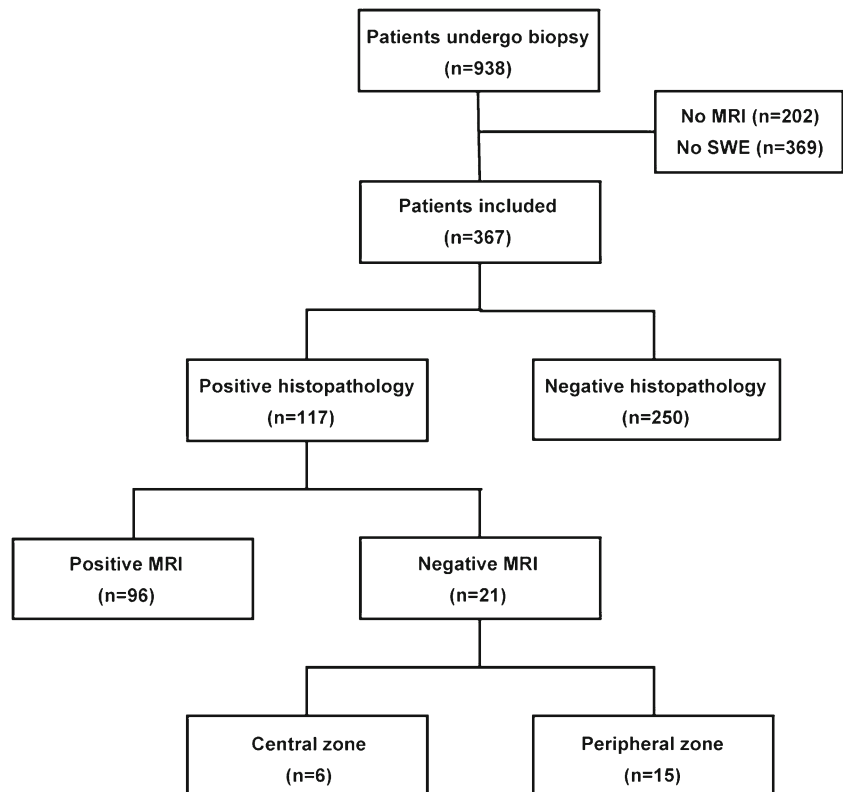
PCa markers

For the positive prostate lesions, significant differences were seen in age ($p = 0.007$) but not seen in V ($p = 0.109$), PSA ($p = 0.197$), fPSA ($p = 0.177$), fPSA/PSA ($p = 0.787$), and PSAD ($p = 0.486$) between the patients with positive and negative MRI (Table 2).

SWE

Eleven of the 117 positive lesions were located in the central zone and thus were excluded for SWE analysis. When performing SWE, there were 83 positive lesions of the 106 lesions considered diagnosed correctly, but 23 lesions missed;

Fig. 1 Flowchart of the patients who underwent prostate biopsy with magnetic resonance imaging and SWE



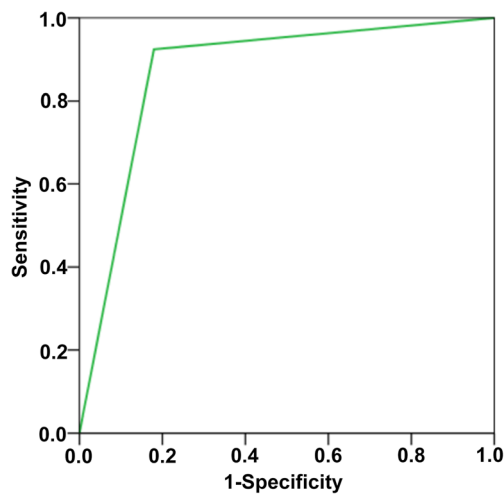


Fig. 2 Receiver operating characteristics analysis of the magnetic resonance imaging for diagnosing clinically significant prostate cancers. The area under the curve was 0.872 (0.827–0.917), which shows significant association with the clinically significant prostate cancers and other prostate lesions ($p < 0.001$)

156 negative lesions of the 250 lesions considered were evaluated correctly, but 94 were overdiagnosed. Therefore, sensitivity was 78.30%, specificity was 62.40%, PPV was 46.90%, NPV was 87.15%, and AUC was 0.704 (95%CI 0.645–0.763) ($p < 0.001$) for SWE and 85.85%, 92.40%, 82.73%, 93.90%, and 0.891 (95%CI 0.848–0.934), respectively, for MRI ($p < 0.001$).

MRI + SWE

When considering MRI + SWE (either the MRI or SWE was positive), 101 positive lesions of the 106 lesions considered were diagnosed correctly, but five lesions were missed; 145 negative lesions of the 250 lesions considered were evaluated correctly, with 105 being overdiagnosed, resulting in sensitivity of 95.28%, specificity of 58.00%, PPV of 49.03%, NPV of 96.67%, and AUC of 0.766 (95%CI 0.717–0.815) ($p < 0.001$). A significant difference was observed when comparing MRI and SWE ($p < 0.001$). The difference was also

significant when comparing MRI + SWE with MRI and SWE, respectively ($p < 0.001$) (Table 3). Supplementary Table S1 shows the features of the 21 patients with positive histopathology but negative MRI. Among them, 15 had PI-RADS 2 lesions and six had PI-RADS 3 lesions; 15 prostates displayed positive histopathological findings in the peripheral zone and six in the central zone. There were five lesions with positive DCE: four PI-RADS 2 and one PI-RADS 3; two lesions showed an abnormal signal in the seminal vesicle. All 21 lesions showed negative lymph nodes.

Qualitative and quantitative SWE in negative MRI

Among the 15 positive prostates of the peripheral zone with negative MRI, qualitative SWE detected 10 patients as malignant and quantitative SWE detected the same 10 patients ($p > 0.05$). When considering the sextant of the peripheral zone, there were six zones that were diagnosed correctly as positive, but 39 were missed; 32 zones of the 45 zones considered were evaluated correctly as negative, with 13 being overdiagnosed with the qualitative measurement, thus representing a sensitivity of 13.33%, specificity of 71.11%, and AUC of 0.422 (0.304–0.541). Using quantitative SWE, eight zones were diagnosed correctly as positive, but 37 were missed; 35 zones of the 45 zones considered were diagnosed correctly as negative, but 10 were overdiagnosed, resulting in a sensitivity of 17.78%, specificity of 77.78%, and AUC of 0.478 (0.358–0.598). There was no significant difference between qualitative and quantitative SWE in sensitivity ($p = 0.500$) with kappa of 0.831 ($p < 0.001$), specificity ($p = 0.549$) with kappa of 0.361 ($p = 0.014$), and AUC ($p = 1.000$) with kappa of 0.558 ($p < 0.001$). There were no significant associations between the Gleason score and qualitative SWE ($p = 0.071$) and quantitative SWE ($p = 0.598$) (Table 4).

As for the positive prostate lesions with negative MRI, no significant differences were observed for age ($p = 0.099$), V ($p = 0.206$), PSA ($p = 0.254$), fPSA ($p = 0.768$), and fPSA/PSA ($p = 0.254$) between SWE-positive and SWE-negative groups, except for PSAD ($p = 0.019$) (Table 5).

Table 2 Comparison of the characteristics of the clinically significant prostate cancer according to the MRI status

Factors	All prostate lesions	All significant prostate cancer lesions	MRI		<i>p</i> value
			Positive	Negative	
Age (years)	67 (29–88)	71 (55–88)	72 (55–88)	66 (58–79)	0.007
V (cm ³)	44.46 (9.28–203.34)	35.35 (15.72–164.42)	36.37 (15.72–164.42)	31.81 (18.72–95.53)	0.109
PSA (ng/ml)	10.28 (0.43–95.12)	15.56 (0.43–95.12)	16.26 (0.43–95.12)	14.69 (5.37–63.85)	0.197
fPSA (ng/ml)	1.40 (0.07–35.72)	1.72 (0.07–35.72)	1.92 (0.07–35.72)	1.58 (0.65–6.72)	0.177
fPSA/PSA	0.14 (0.01–0.67)	0.11 (0.01–0.67)	0.11 (0.01–0.67)	0.11 (0.03–0.35)	0.787
PSAD (ng/ml/cm ³)	0.21 (0.01–3.96)	0.40 (0.01–3.96)	0.40 (0.01–3.96)	0.43 (0.11–1.00)	0.486

MRI, magnetic resonance imaging; V, volume of the prostate gland; PSA, prostate-specific antigen; fPSA, prostate-specific antigen; PSAD, prostate-specific antigen density

Representative cases

Supplementary Figs. S1–S3 present representative cases.

Discussion

MRI and SWE can be used for the diagnosis of sPCa [7, 8, 11, 14], but they show some misdiagnosis. MRI plays an important role in prostate diagnosis and many studies revealed the efficiency and significance of the MRI [1, 4, 13, 15–17]. Although there are differences between versions 1 and 2 of PI-RADS, both of them were proven to be helpful in prostate diagnosis [9, 18–22]. MRI is able to detect sPCa (44–87%) with a high NPV (63–98%) [17, 23, 24]. Nevertheless, a previous study showed that clinically important lesions can be missed or their size can be underestimated at MRI [5]. The present study showed that the sensitivity of MRI was 82.1%, which was basically similar with those previous studies. Combining MRI with other imaging modalities such as SWE could decrease the misdiagnosis rate.

Even before the appearance of morphological variation detected by the examinations such as MRI and US, the hardness of the prostate tissue changes early with the desmoplastic reaction or the infiltration of cancer cells into the interstitial tissues, leading to sPCa tissues being stiffer than normal tissues [25–27]. Both strain elastography and SWE are helpful to detect stiff prostatic tissues [27–32]. SWE even allows the quantitative measurements of prostate tissue stiffness, which showed hopeful preliminary findings in the characterization and detection of sPCa [6, 32, 33]. In the present study, the diagnostic value of SWE alone was lower than MRI alone, which was expected since the tissue elasticity examination is affected by many factors and is user-dependent.

When considering the combination of MRI and SWE, the sensitivity was higher than with MRI or SWE alone, which can reduce by almost 10% the missed diagnosis of cancerous prostate lesions while increasing misdiagnosis by almost 30%, thus resulting in a lower AUC than MRI alone (0.766 vs. 0.891). It may be another evidence why the MRI plays the most important role in diagnosing prostate cancer. The aim of

Table 4 Diagnostic value of shear-wave elastography in the qualitative and quantitative modes for patients with clinically significant prostate cancers but negative MRI

Indexes	Qualitative SWE	Quantitative SWE	p value	Kappa
Sensitivity (%)	13.33	17.78	0.500	0.831
Specificity (%)	71.11	77.78	0.549	0.361
AUC	0.578	0.522	1.000	0.558

MRI, magnetic resonance imaging; SWE, shear-wave elastography; AUC, area under the curve

this subject is analyzing the value of SWE for the clinically significant prostate cancer with false-negative MRI results rather than the diagnostic value of SWE + MRI. Prostate biopsy is conducted for many suspicious signs while negative results of both SWE and MRI could not influence biopsy determination. Adding SWE to MRI can give more information for biopsy.

In the present study, there was no significant difference in all of the factors (aside from age) such as V, PSA, fPSA, fPSA/PSA, and PSAD for positive prostate tissues between the positive and negative MRI groups. Schouten et al [34] revealed that sPCa lesions missed by MR-Bx most often had involvement of the dorsolateral (58%) and apical (37%) segments. There is little study focusing on the difference of sPCa between the positive and negative MRI.

The present study showed that both qualitative and quantitative measurements could detect 10 patients with sPCa from 15 patients with negative MRI, but this detection was not associated with the cancer subtype, although this could be due to the small number of patients.

This study had limitations. Firstly, the sample size was small, which might hide significant results. MRI detected a large number of sPCa and only a small number of sPCa were missed by MRI, which could explain why there are few studies focusing on sPCa with false-negative MRI results. Secondly, we did not analyze the sPCa of the central zone as the SWE examination was only performed in the peripheral zone, because SWE imaging is influenced by tissue calcification, imaging depth, and probe pressure. There are some systems (such as the GE system) that can perform SWE of

Table 3 Diagnostic value of different imaging modalities for clinically significant prostate cancer of 356 patients

Modality	Sensitivity (%)	Specificity (%)	PPV (%)	NPV (%)	AUC (95%CI)	p*
MRI	85.85	92.40	82.73	93.90	0.89 (0.85–0.93)	<0.001
SWE	78.30	62.40	46.90	87.15	0.70 (0.65–0.76)	<0.001
MRI + SWE	95.28	58.00	49.03	96.67	0.77 (0.72–0.82)	<0.001

SWE could not be applied to the central zone lesions and 11 patients were excluded from the original 367 MRI, magnetic resonance imaging; SWE, shear-wave elastography; PPV, positive predictive value; NPV, negative predictive value; AUC, area under the curve

*Compared with the histopathological findings

Table 5 Comparison of the characteristics of the clinically significant prostate cancers among patients with negative MRI and according to SWE

Factors	All malignant lesions	SWE		<i>p</i>
		Detected	Ignored	
Age (years)	66.00 (58–75)	66.00 (58–75)	70.00 (65–75)	0.099
V (cm ³)	29.08 (18.72–95.53)	31.70 (23.89–95.53)	28.08 (18.72–40.70)	0.206
PSA (ng/ml)	12.35 (5.48–32.12)	10.02 (5.48–28.63)	18.76 (5.53–32.12)	0.254
fPSA (ng/ml)	1.58 (0.25–6.72)	1.53 (0.25–6.72)	1.72 (0.47–2.59)	0.768
fPSA/PSA	0.12 (0.04–0.35)	0.12 (0.05–0.35)	0.08 (0.04–0.14)	0.254
PSAD (ng/ml/cm ³)	0.35 (0.11–1.00)	0.22 (0.11–0.76)	0.79 (0.23–1.00)	0.019

V, volume of the prostate gland; PSA, prostate-specific antigen; fPSA, prostate-specific antigen; PSAD, prostate-specific antigen density

the entire prostate, but the system used in the present study only performs well in a shallow depth and thus is unable to meet this requirement. In addition, different SWE thresholds have to be applied for different regions of the prostate for the diagnosis of prostate diseases. Calculation for different parts separately greatly increases the complexity of the analyses. Therefore, only the peripheral zone was imaged in the present study. Thirdly, the SWE examination and the biopsy were conducted using different machines, which might cause some mismatching of the SWE findings with the histopathological results. sPCa is different from many other malignant tumors as most of the other tumors show apparent mass that could be matched between SWE and US. In our study, SWE imaging was only performed in the sextant zone as SWE imaging of the entire prostate continuously is too difficult to acquire. Even when scanning the stiffness of the prostate slowly, we cannot match the SWE with US well enough to gain accurate biopsy. Fourthly, participants with PSA > 100 ng/ml were excluded in this study since the fPSA/PSA cannot be measured and thus the diagnostic value could be reduced as the incidence of sPCa is very high in this group. Finally, there are many other diagnostic modalities used for the diagnosis of prostatic tissues such as radiomics, which might play a more important role than MRI. In addition, MRI-US-guided biopsy might be more effective than TRUS-Bx, while in our study we only used MRI and TRUS-Bx.

In conclusion, the results strongly suggest that adding SWE to MRI in patients with negative MRI for prostate examination could allow the correct diagnosis of additional patients and reduce the false-negative rate. SWE plays an important role in the detection of sPCa in prostates with false-negative MRI results. SWE might reduce the false-negative rate of MRI. More studies with a larger sample size and focusing on prostate elastography are needed.

Funding This study has received funding through Grant SHDC12016233 from the Shanghai Hospital Development Center, Grant 17411967400 from the Science and Technology Commission of Shanghai Municipality, and Grants 81471673 and 81671699 from the National Natural Science Foundation of China.

Compliance with ethical standards

Guarantor The scientific guarantor of this publication is Rong Wu.

Conflict of interest The authors of this manuscript declare no relationships with any companies, whose products or services may be related to the subject matter of the article.

Statistics and biometry No complex statistical methods were necessary for this paper.

Informed consent Written informed consent was obtained from all subjects (patients) in this study.

Ethical approval Institutional Review Board approval was obtained.

Methodology

- retrospective
- diagnostic or prognostic study
- performed at one institution

References

1. Leslie SW, Soon-Sutton TL, Siref LE (2017) Cancer, prostate. StatPearls. StatPearls Publishing, Treasure Island (2017) Cancer, prostate. StatPearls. StatPearls Publishing StatPearls Publishing LLC, Treasure Island
2. Zheng R, Zeng H, Zhang S, Chen W (2017) Estimates of cancer incidence and mortality in China, 2013. *Chin J Cancer* 36:66
3. Wong MC, Goggins WB, Wang HH et al (2016) Global incidence and mortality for prostate cancer: analysis of temporal patterns and trends in 36 countries. *Eur Urol* 70:862–874
4. Weinreb JC, Barentsz JO, Choyke PL et al (2016) PI-RADS Prostate Imaging - Reporting and Data System: 2015, version 2. *Eur Urol* 69:16–40
5. Borofsky S, George AK, Gaur S et al (2018) What are we missing? False-negative cancers at multiparametric MR imaging of the prostate. *Radiology* 286:186–195
6. Correas JM, Tissier AM, Khairoune A et al (2015) Prostate cancer: diagnostic performance of real-time shear-wave elastography. *Radiology* 275:280–289
7. Woo S, Suh CH, Kim SY, Cho JY, Kim SH (2017) Shear-wave elastography for detection of prostate cancer: a systematic review and diagnostic meta-analysis. *AJR Am J Roentgenol* 209:806–814

8. Sang L, Wang XM, Xu DY, Cai YF (2017) Accuracy of shear wave elastography for the diagnosis of prostate cancer: a meta-analysis. *Sci Rep* 7:1949
9. Hamoen EJJ, de Rooij M, Witjes JA, Barentsz JO, Rovers MM (2015) Use of the Prostate Imaging Reporting and Data System (PI-RADS) for prostate cancer detection with multiparametric magnetic resonance imaging: a diagnostic meta-analysis. *Eur Urol* 67:1112–1121
10. Niu XK, Chen XH, Chen ZF, Chen L, Li J, Peng T (2018) Diagnostic performance of biparametric MRI for detection of prostate cancer: a systematic review and meta-analysis. *AJR Am J Roentgenol* 211:369–378
11. Tan CH, Wei W, Johnson V, Kundra V (2012) Diffusion-weighted MRI in the detection of prostate cancer: meta-analysis. *AJR Am J Roentgenol* 199:822–829
12. Su R, Xu G, Xiang L, Ding S, Wu R (2018) A novel scoring system for prediction of prostate cancer based on shear wave elastography and clinical parameters. *Urology* 121:112–117
13. Furlan A, Borhani AA, Westphalen AC (2018) Multiparametric MR imaging of the prostate: interpretation including Prostate Imaging Reporting and Data System version 2. *Radiol Clin North Am* 56:223–238
14. de Rooij M, Hamoen EH, Fütterer JJ, Barentsz JO, Rovers MM (2014) Accuracy of multiparametric MRI for prostate cancer detection: a meta-analysis. *AJR Am J Roentgenol* 202:343–351
15. Mazaheri Y, Akin O, Hricak H (2017) Dynamic contrast-enhanced magnetic resonance imaging of prostate cancer: a review of current methods and applications. *World J Radiol* 9:416–425
16. Nazim SM, Ather MH, Salam B (2018) Role of multi-parametric (mp) MRI in prostate cancer. *J Pak Med Assoc* 68:98–104
17. Abd-Alazeez M, Kirkham A, Ahmed HU et al (2014) Performance of multiparametric MRI in men at risk of prostate cancer before the first biopsy: a paired validating cohort study using template prostate mapping biopsies as the reference standard. *Prostate Cancer Prostatic Dis* 17:40–46
18. Benndorf M, Waibel L, Krönig M, Jilg CA, Langer M, Krauss T (2018) Peripheral zone lesions of intermediary risk in multiparametric prostate MRI: frequency and validation of the PI-RADSV2 risk stratification algorithm based on focal contrast enhancement. *Eur J Radiol* 99:62–67
19. Zuo MZ, Zhao WL, Wei CG et al (2017) Preliminary applicability evaluation of Prostate Imaging Reporting and Data System version 2 diagnostic score in 3.0T multi-parameters magnetic resonance imaging combined with prostate specific antigen density for prostate cancer. *Zhonghua Yi Xue Za Zhi* 97:3693–3698
20. Krishna S, McInnes M, Lim C et al (2017) Comparison of Prostate Imaging Reporting and Data System versions 1 and 2 for the detection of peripheral zone Gleason score 3 + 4 = 7 cancers. *AJR Am J Roentgenol* 209:W365–w373
21. Becker AS, Cornelius A, Reiner CS et al (2017) Direct comparison of PI-RADS version 2 and version 1 regarding interreader agreement and diagnostic accuracy for the detection of clinically significant prostate cancer. *Eur J Radiol* 94:58–63
22. Polanc S, Helbich TH, Bickel H et al (2016) Head-to-head comparison of PI-RADS v2 and PI-RADS v1. *Eur J Radiol* 85:1125–1131
23. Fütterer JJ, Briganti A, De Visschere P et al (2015) Can clinically significant prostate cancer be detected with multiparametric magnetic resonance imaging? A systematic review of the literature. *Eur Urol* 68:1045–1053
24. Thompson JE, van Leeuwen PJ, Moses D et al (2016) The diagnostic performance of multiparametric magnetic resonance imaging to detect significant prostate cancer. *J Urol* 195:1428–1435
25. Harvey H, Morgan V, Fromageau J, O’Shea T, Bamber J, deSouza NM (2018) Ultrasound shear wave elastography of the normal prostate: interobserver reproducibility and comparison with functional magnetic resonance tissue characteristics. *Ultrasound Imaging* 161734618754487. <https://doi.org/10.1177/0161734618754487>
26. Hoyt K, Castaneda B, Zhang M et al (2008) Tissue elasticity properties as biomarkers for prostate cancer. *Cancer Biomark* 4:213–225
27. Good DW, Stewart GD, Hammer S et al (2014) Elasticity as a biomarker for prostate cancer: a systematic review. *BJU Int* 113: 523–534
28. Salomon G, Köllerman J, Thederan I et al (2008) Evaluation of prostate cancer detection with ultrasound real-time elastography: a comparison with step section pathological analysis after radical prostatectomy. *Eur Urol* 54:1354–1362
29. Walz J, Marcy M, Pianna JT et al (2011) Identification of the prostate cancer index lesion by real-time elastography: considerations for focal therapy of prostate cancer. *World J Urol* 29:589–594
30. Brock M, von Bodman C, Palisaar RJ et al (2012) The impact of real-time elastography guiding a systematic prostate biopsy to improve cancer detection rate: a prospective study of 353 patients. *J Urol* 187:2039–2043
31. Bercoff J, Tanter M, Fink M (2004) Supersonic shear imaging: a new technique for soft tissue elasticity mapping. *IEEE Trans Ultrason Ferroelectr Freq Control* 51:396–409
32. Barr RG, Memo R, Schaub CR (2012) Shear wave ultrasound elastography of the prostate: initial results. *Ultrasound Q* 28:13–20
33. Zhang M, Wang P, Yin B, Fei X, Xu XW, Song YS (2015) Transrectal shear wave elastography combined with transition zone biopsy for detecting prostate cancer. *Zhonghua Nan Ke Xue* 21: 610–614
34. Schouten MG, van der Leest M, Pokorny M et al (2017) Why and where do we miss significant prostate cancer with multi-parametric magnetic resonance imaging followed by magnetic resonance-guided and transrectal ultrasound-guided biopsy in biopsy-naive men? *Eur Urol* 71:896–903

Publisher’s note Springer Nature remains neutral with regard to jurisdictional claims in published maps and institutional affiliations.